

Microbial Dysbiosis in the Lung and Gut in Response to Inhalable Particulate Matters in Pneumoconiosis Patients and Animals

Huimin Ma, Zheng Dong,* Xu Zhang, Ning Li, Conghe Liu, Xi Zhou, Jin He, Juan Ma, Shuping Zhang, Haidong Kan, and Sijin Liu



Cite This: *Environ. Sci. Technol.* 2025, 59, 10826–10840



Read Online

ACCESS |

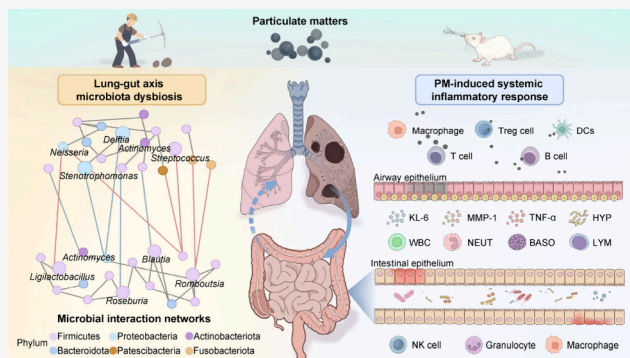
Metrics & More

Article Recommendations

Supporting Information

ABSTRACT: Pneumoconiosis is a progressive and life-threatening fibrotic lung disorder caused by the prolonged deposition of inhaled particulate matters (PMs); thus far, no cure is available. Emerging evidence has suggested that the resulting disordered respiratory microbiome is caused by disturbed lung architecture and homeostasis responding to inhalable PMs. Lung microbiome dysbiosis also contributes to injury to the lung and distant organs, such as the intestine, through the lung–gut axis. Current studies on the microbiome–disease interplay are still in their infancy, and sufficient understanding of microbial heterogeneity in pathological processes is lacking. Here we investigated the microbiome in the lung and gut of patients with pneumoconiosis in comparison to healthy individuals. Our findings indicated reciprocal causation between lung injuries and microbial dysbiosis under particle exposure; pulmonary *Streptococcus* and *Stenotrophomonas*, along with intestinal *Ligilactobacillus* and *Blautia*, may represent key microbial communities influencing pneumoconiosis progression. We defined close microbiota crosstalk between the lung and gut, as evidenced by their interaction networks, implying considerable effects on the gut microenvironment through either direct microbial translocation or other mechanisms such as inflammation-driven alterations. Animal experiments further corroborated the findings in humans. Collectively, our results highlight the potential involvement of the lung–gut axis microbial dysbiosis in pneumoconiosis pathogenesis and open a new avenue to develop microbiome-targeted diagnosis and treatment strategies.

KEYWORDS: Inhalable particulate matters, pneumoconiosis, lung–gut axis, microbial dysbiosis, systemic inflammation



1. INTRODUCTION

Occupational exposure is a typical instance of long-term exposure to inhalable particulate matters (PMs), posing a profound threat to public health. Mineral particles are predominant in the occupational exposure, including coal dust, silica dust, and asbestos fibers, which are mainly composed of heavy metal components, inorganic salt ions, and organic carbon.^{1,2} Among all potential routes of exposure, the respiratory system is the most vulnerable to exogenous particles, owing to its extensive surface area that is in direct contact with the environment.^{3,4} Once inside the body, these inhaled particles could penetrate the air-blood barrier and cause toxic effects on distant organs through oxidative stress, genetic damage, and immune toxicity.⁵ As the most prevalent occupational disease worldwide, PM-caused pneumoconiosis could significantly undermine the quality and longevity of life; its progression continues to deteriorate even after patients are withdrawn from occupational exposure.^{6,7} To date, the pathogenesis, complications, and prevention of pneumoconiosis remain unclear. Our previous study reported the characteristics of the upper respiratory microbiota imbalances

in patients with stage I pneumoconiosis, which inspired us to continue the study of host-microbiome interactions in particle-induced respiratory and extrapulmonary impairment.⁸

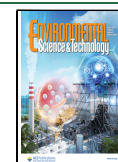
According to the current knowledge, the host microbiome dictates general homeostasis in maintaining health or preventing diseases.^{9,10} The microbiota greatly influences the regulation of host immune responses and metabolic processes,^{11,12} and its dysbiosis can trigger various diseases, ranging from gastrointestinal to respiratory, neurological, inflammatory, liver, and cardiovascular diseases.^{13–16} Close associations have been demonstrated by epidemiological and toxicological studies between increases in exogenous particle concentrations and changes in respiratory microbiota.^{17,18} Inhalable PMs would disrupt the relatively stable community

Received: January 16, 2025

Revised: May 10, 2025

Accepted: May 12, 2025

Published: May 29, 2025



composition of the lung microbiota by causing oxidative stress and inflammation, giving rise to disordered microbial metabolism.¹⁹ Additionally, growing evidence from both human and animal studies has stressed the potential impacts of inhalable particles on gut microbiota, and the metabolites produced by the altered gut microbiome could reversely shape systemic immunity.^{20–22} Despite these progresses, the microbiota cross-talk between the lung and intestine, particularly how it changes under exposure to PMs remains unclear.^{23–26} Filling these gaps in knowledge is crucial to understanding the synergistic effects of PM exposure and microbiome disturbance on host health or disease.

Previous investigations into the microbiota of patients with pneumoconiosis have predominantly concentrated on the respiratory system, and knowledge regarding intestinal microbiota alterations and the interactions occurring along the lung–gut axis remains scarce.⁸ Here, we aimed to shed light on the lung–gut axis microbiome crosstalk in response to PMs by recruiting a group of pneumoconiosis patients and examining concurrently collected specimens from both the lung and gut. The pneumoconiosis patients exhibited a shifted microbiome profile in the pulmonary and intestinal tracts relative to healthy controls, indicative of an ecological dysbiosis characterized by altered microbial α -diversity, deviated microbial community, and different representative taxa. We further confirmed the dysbiosis of the lung–gut microbial axis in patients and mice with pneumoconiosis, which was closely associated with PM-induced systemic inflammatory responses. Together, our findings provide a deeper understanding of the lung–gut microbial crosstalk, contributing to more effective utilization of the host microbiome in the prophylaxis, diagnosis, and treatment of pulmonary disorders.

2. MATERIALS AND METHODS

2.1. Study Population and Microbiota Sample Collection. The study was approved by the Ethics Review Committee of Shandong First Medical University (approval number: R202306270137). Twenty patients with pneumoconiosis (male, average age: 55 years) were recruited at the Occupational Diseases Hospital of Shandong First Medical University. All patients were diagnosed with pneumoconiosis during outpatient visits by high-resolution computed tomography (CT) scanning of the thorax (Canon, Japan). Twenty healthy staff members from the hospital logistics department were recruited as a control group (male, average age: 51 years). Exclusion criteria encompassed any recorded gastrointestinal disorders, such as intestinal malignancies or active gastrointestinal infections; participants undergoing chemotherapy and those with acute and/or recent infections necessitating short-term antibiotic treatment (oral or intravenous) within the past 1 month were also excluded. Additionally, both groups reported no alcohol consumption history within 1 week prior to the study. Smoking history was documented in 7 participants from the pneumoconiosis group in contrast to 5 in the control group, with no statistically significant difference between the two groups.

All volunteers signed informed consent with full understanding of the research content and purpose. Standardized sputum and stool samples were collected between 8:00–9:00 a.m. following a minimum 12 h fasting period. All biological specimens were routinely preserved at 4 °C immediately after collection, followed by standard aliquoting and –80 °C cryopreservation within 2 h postcollection.

2.2. Animal Model of Pneumoconiosis. The animal experimental protocols were approved by the Ethics Review Committee of Shandong First Medical University (approval number: W202306270278). Seven-week-old female BALB/c mice were acquired from the Vital River Laboratory Animal Technology Co., Ltd. (Beijing, China). The experimental group mice (PM group) were intranasally administered with 1 mg/kg body weight inhalable PMs once every 48 h for a total of 18 days. After being anaesthetized by respiration, micro-CT images of the lungs were obtained using a Quantum GX2Micro CT instrument (PerkinElmer, China).

The mice were weighed daily and euthanized on the 18th day. Afterward, peripheral blood was assayed with a hematology analyzer (BC-5130, Mindray, Ltd., China). Portions of the lung and colon were fixed in 4% paraformaldehyde solution for tissue sectioning and staining. Lung sections were stained with hematoxylin and eosin (H&E) and Masson stains. Duodenal segments were collected, Swiss-rolled, and stained with H&E and periodic acid-Schiff (PAS). All sections were scanned using an inverted light microscope at 10 \times and 20 \times magnification.²⁷

Immune cell populations in lung and gut tissues were determined by an Attune NxT flow cytometry platform (Thermo Fisher Scientific, USA). In brief, single-cell suspensions were prepared and stained with fluorescence-conjugated antibodies for subsequent flow cytometry analysis, as documented in prior studies.^{5,27} Detailed information about the antibodies is listed in Table S1.

2.3. Measurements of Serum Parameters. Commercial enzyme-linked immunosorbent assay (ELISA) kits were utilized to quantify pneumoconiosis biomarkers in the serum of patients or mice. These testing kits included Krebs von den Lungen-6 (KL-6) ELISA kits (Mlbio, China), matrix metalloproteinase-1 (MMP-1) ELISA kits (ABclonal, China), tumor necrosis factor- α (TNF- α) ELISA kits (ABclonal, China), and hydroxyproline (HYP) ELISA kits (Solarbio, China).

2.4. Characterization of Bronchoalveolar Lavage Fluid (BALF). To confirm the presence of bacteria in the lung, we conducted fluorescence *in situ* hybridization (FISH) on BALF from patients with pneumoconiosis and healthy volunteers. PMs in BALF of pneumoconiosis patients were observed using a transmission electron microscopy (TEM, Hitachi, Japan), and the elemental composition was determined using energy-dispersive spectrometry (EDS) (Thermo Fisher Scientific, USA).^{28,29}

2.5. DNA Extraction and Sequencing. Sequencing of 16S rRNA gene was performed by Novogene (Beijing, China). After DNA extraction, PCR amplification was conducted on DNA samples utilizing the universal primers 515F-806R targeting the V4 region of the bacterial 16S rRNA gene, employing Phusion High-Fidelity PCR Master Mix (BioLabs, USA).³⁰ Sequencing libraries were generated, indexed, and pooled according to effective concentration and required data volume, and sequenced on Illumina platforms. The initial amplicon sequence variants (ASVs) for the previously acquired effective tags were derived by denoising through the DADA2 algorithm or the *deblur* module within QIIME2 (version QIIME2–202202).³¹ The absolute abundance of ASVs was standardized by utilizing the sample with the lowest sequence count as the standard sequence number.³²

2.6. Microbiota Statistical Analysis. The α -diversity indices, including observed operational taxonomic units (OTUs), Shannon, Chao1, and Simpson's indices; β -diversity

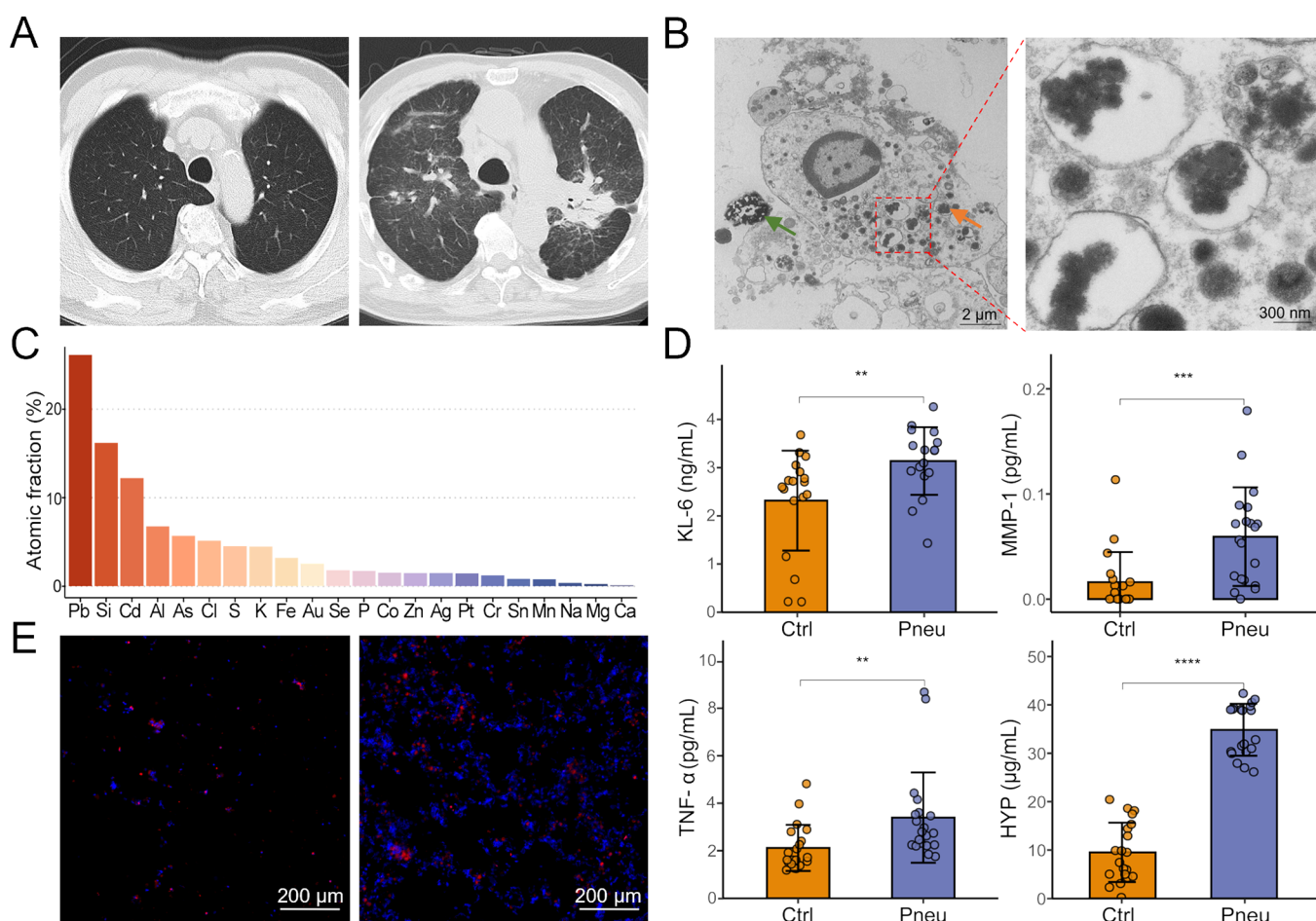


Figure 1. Particle deposition and bacterial burden in the lower respiratory tract of patients with pneumoconiosis. (A) Representative CT images of the healthy control and pneumoconiosis groups. (B) Representative TEM image of the BALF of a pneumoconiosis patient. The orange arrowheads denote the accumulated PMs, and the green arrowheads indicate bacteria. (C) Elemental composition and proportion of particles in BALF of pneumoconiosis patients were detected by energy-dispersive spectrometry. (D) Values of KL-6, MMP-1, TNF- α , and HYP in the serum of the two groups. (E) Fluorescence FISH analysis of BALF from control volunteers and pneumoconiosis patients. Bacterial 16S rRNA is stained with EUB338 probe (red), and cell nuclei are stained with DAPI (blue, 4',6-diamidino-2-phenylindole). Ctrl, healthy control. Pneu, pneumoconiosis. (***) indicates $P < 0.01$, (***) denotes $P < 0.001$, and (****) denotes $P < 0.0001$, as indicated.

analyses, including principal coordinates analysis (PCoA) and partial least-squares discriminant analysis (PLS-DA); and species composition histograms (at the phylum and genus levels) were computed using the *vegan* package in R (4.2.0). Results were plotted using the *ggplot2* package. Differential taxa analyses were performed using linear discriminant analysis (LDA) and effect size (LEfSe) between the control groups and experimental groups, and the LDA results obtained for the differential genera were plotted using the *ggplot2* package in R.³³ Interactome networks were obtained based on Spearman's correlation coefficients, displaying the solid line co-occurrence network using Gephi (0.9.2). The interaction network consists of lung and gut microbiota bidirectional interaction hooked up by interconnecting lines between them.²³ The connecting lines represent bacterial genera exhibiting significant correlations between these two ecological niches ($|r| \geq 0.6$, $P < 0.05$), with red lines indicating positive correlations and blue lines denoting negative correlations. The Mantel test results between pneumoconiosis indicators (KL-6, MMP-1, TNF- α , and HYP) and microbial abundance were obtained using the *vegan* package in R.

3. RESULTS

3.1. Pneumoconiosis Patients Exhibited Particle Deposition Accompanied by Aggravated Bacterial Burden in the Lung

Patients with pneumoconiosis included in this study all originated from the same gold mine located in Shandong, China. They underwent comprehensive clinical evaluation and imaging examinations. Regarding CT examination, the lung window of the control group displayed clear lung textures with normal direction and distribution, and no atypical density opacities were detected in the pulmonary field (Figure 1A). The lung texture of the pneumoconiosis patient was irregularly thick, with several visible high-density shadows of varied sizes in the lung field accompanied by frosted glass shadows. Cells extracted from BALF of pneumoconiosis patients were fixed and photographed with TEM, where agglomerated inhalable PMs were observed both extracellularly and intracellularly (Figure 1B). The PMs elemental composition included harmful metallic elements, such as plumbum (Pb), silicon (Si), cadmium (Cd), aluminum (Al), and arsenic (As), as well as potentially harmful metallic elements such as Aurum (Au), selenium (Se), cobalt (Co), argentum (Ag), chromium (Cr), and stannum (Sn) (Figure 1C).

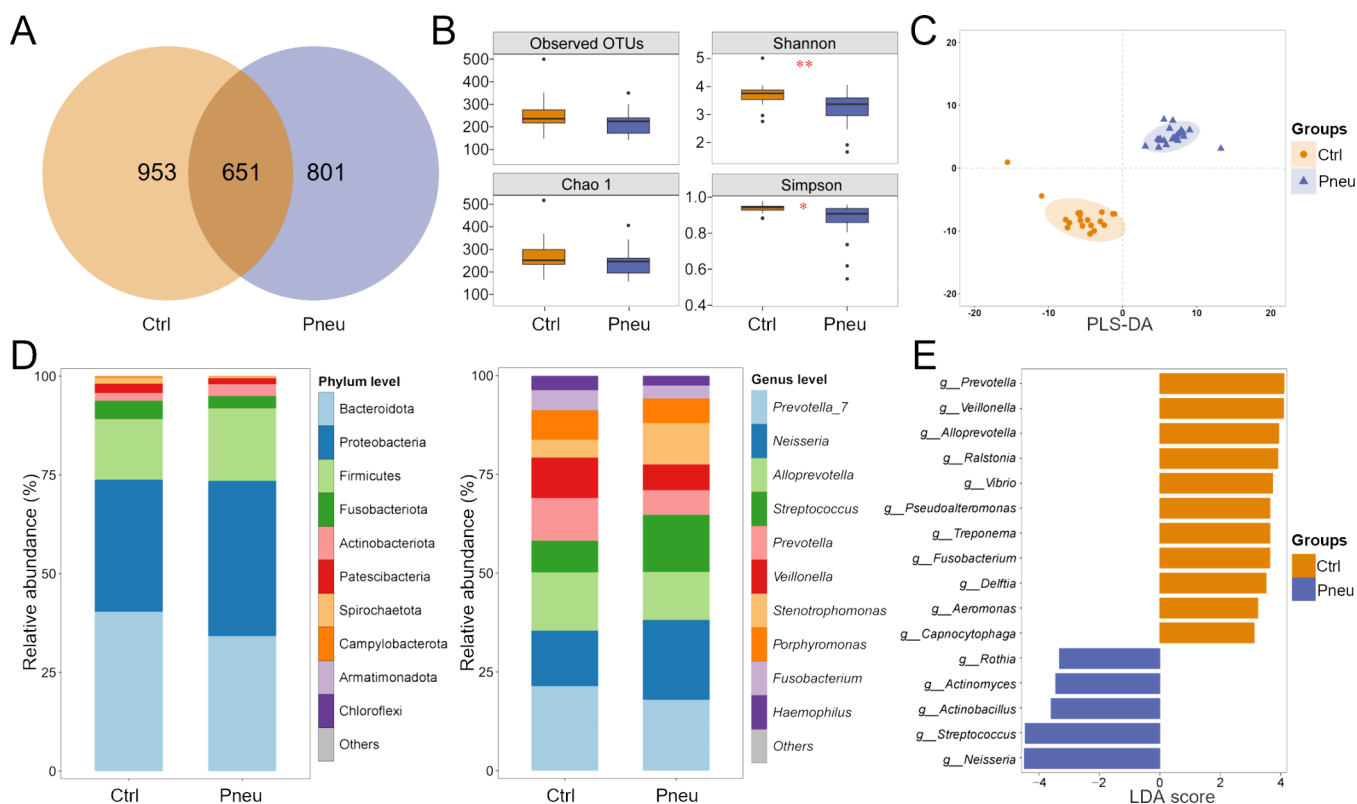


Figure 2. Lung microbiota composition and diversity of pneumoconiosis patients and healthy controls. (A) Venn diagrams showing unique alterations in ASVs between the two groups. (B) α -Diversity and (C) β -diversity of the microbial communities in the sputum of the healthy control group ($n = 20$) and pneumoconiosis group ($n = 20$). (D) Relative abundance of bacteria at the phylum and genus levels in the two groups. (E) LEfSe analysis of bacterial species with significant differences at the genus level. (*) indicates $P < 0.05$ and (**) indicates $P < 0.01$, as indicated.

According to previous studies, KL-6, TNF- α , MMP-1, and HYP could serve as biomarkers to assist in the diagnosis of pneumoconiosis.^{34–36} The levels of KL-6, MMP-1, TNF- α , and HYP in the serum of patients with pneumoconiosis were significantly higher than those in control individuals (Figure 1D, $P < 0.01$). The average value of KL-6 in the control group was 2.31 ng/mL, while that in patients with pneumoconiosis was 3.14 ng/mL ($P < 0.01$). KL-6 levels sensitively reflect alveolar injury, which can promote fibroblast proliferation and migration, affecting the occurrence and development of fibrosis.^{36,37} MMP-1 was almost undetectable in healthy controls but was largely increased in patients with pneumoconiosis at an average value of 0.06 pg/mL ($P < 0.001$). The MMP enzyme family is considered a potential biomarker in diagnosing and monitoring the progression of various pulmonary fibrotic diseases, with MMP-1 as a key member that plays a crucial role in the degradation of type I collagen.³⁸ The levels of TNF- α and HYP in the serum of patients with pneumoconiosis were approximately 2–3 times greater than those of the healthy controls ($P < 0.01$ and $P < 0.0001$, respectively). The pro-inflammatory factor TNF- α stimulates the local inflammatory responses by promoting the production of superoxides and the release of lysosomal enzymes.³⁹ HYP is a major component of collagen and highly expressed in the serum of patients with lung fibrosis.³⁵ Additionally, the prevalence of HYP in patients with stage III pneumoconiosis was significantly higher than that in stage I patients, indicating that HYP can also assist in the diagnosis of disease staging (Figure S1). Thus, pneumoconiosis could be primarily

characterized by inflammation and fibrosis of the lung, with the degree of fibrosis worsening as the disease progresses.

Our previous studies have shown that occupational exposure to inhalable PMs can alter the microecology of the upper respiratory tract, including multiple ecological niches such as the oral cavity, nasal cavity, and pharynx.⁴⁰ The FISH imaging of cells derived from the BALF of healthy volunteers and pneumoconiosis patients revealed the presence of intact bacteria (Figure 1E). There was also an increased presence of bacteria, as well as a higher number of inflammatory cells or desquamated epithelial cells, in the BALF of patients with pneumoconiosis.

3.2. Differences in Pulmonary Microbiome Profiles between the Healthy Controls and Patients with Pneumoconiosis.

According to the sequencing results, a total of 1,738,508 and 2,134,588 effective tags were obtained from the sputum samples in the control and pneumoconiosis groups, respectively. After denoising and deduplicating using DADA2,⁴¹ 1604 and 1452 ASVs were obtained in the two groups (Figure 2A). The features were categorized into 23 phyla, 38 classes, 84 orders, 138 families, and 220 genera in the control group, with 16 phyla, 24 classes, 55 orders, 95 families, and 165 genera in the pneumoconiosis group.

The α -diversity indices, including the Shannon and Simpson's indices ($P < 0.01$ and $P < 0.05$, respectively), revealed that the diversity and richness of the pulmonary microbiota decreased in patients with pneumoconiosis compared with those in healthy controls (Figure 2B). β -Diversity analysis of the lung microbiota showed a large difference between the two groups (Figure 2C). At the phylum

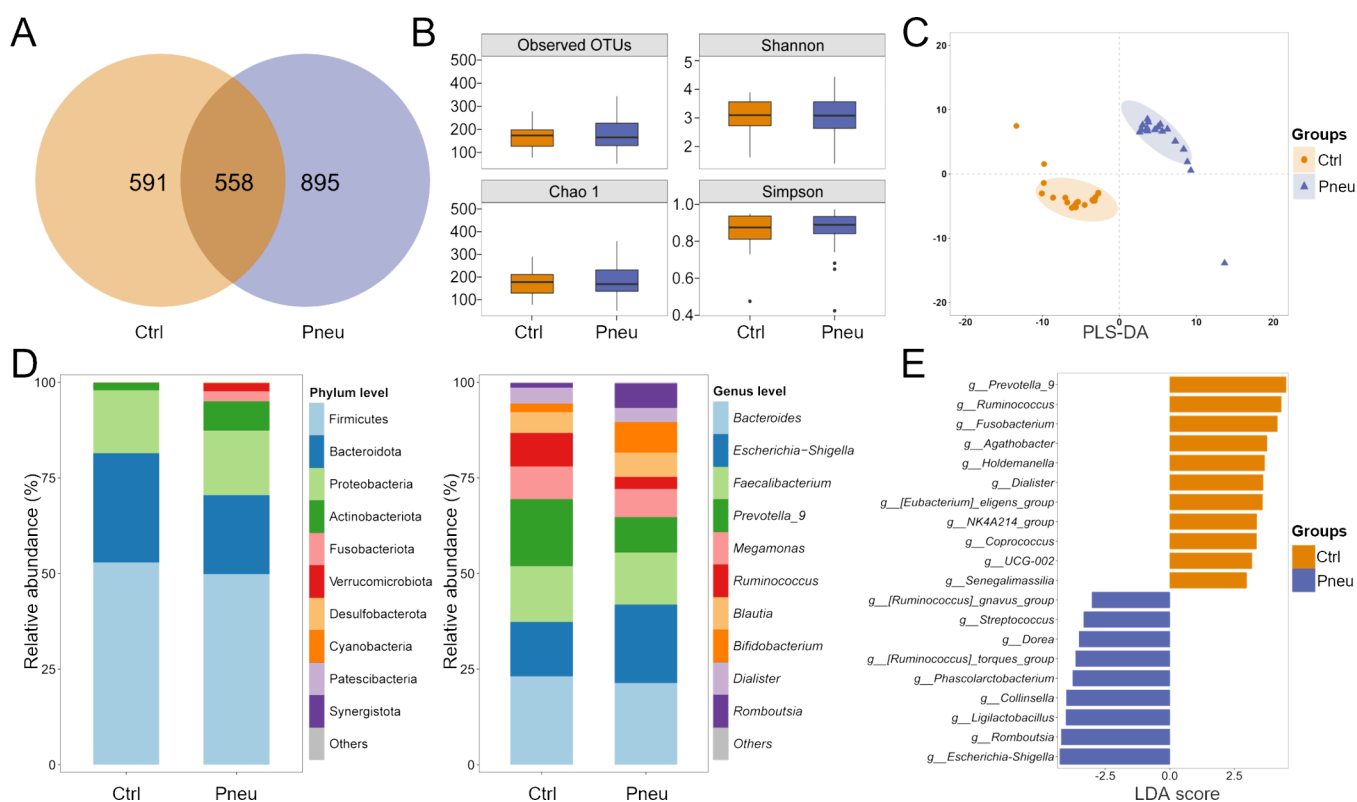


Figure 3. Gut microbiota composition and diversity of pneumoconiosis patients and healthy controls. (A) Venn diagrams showing unique alterations in ASVs between two groups. (B) α -Diversity and (C) β -diversity of the microbial communities in feces specimens of the healthy controls ($n = 20$) and patients with pneumoconiosis ($n = 20$). (D) Relative abundance of bacteria at the phylum and genus levels in the two groups. (E) LefSe analysis of bacterial species with significant differences at the genus level.

level of respiratory bacteria, Proteobacteria, Bacteroidota, and Firmicutes were dominant in the two groups, followed by Fusobacteriota, Actinobacteriota, Patescibacteria, and Spirochaetota (Figure 2D). At the genus level of respiratory bacteria, the top ten bacterial genera in patients with pneumoconiosis accounted for 69.4% of the total sequences, including *Prevotella_7*, *Neisseria*, *Alloprevotella*, *Streptococcus*, *Prevotella*, *Veillonella*, *Stenotrophomonas*, *Porphyrromonas*, *Fusobacterium*, and *Haemophilus*. Compared with that in the healthy individuals, the abundance of normal respiratory bacteria such as *Prevotella*, *Veillonella*, and *Alloprevotella* was decreased, and *Neisseria*, *Streptococcus*, *Actinobacillus*, *Actinomyces*, and *Rothia* were enriched in the sputum flora of patients with pneumoconiosis (Figure 2E, LDA score >3). These shifts indicated the dysbiosis of the lung microbiome in pneumoconiosis patients.

The enrichment of *Neisseria* is associated with 2.25-fold increase in the incidence of severe respiratory symptomatology, including chronic obstructive pulmonary disease (COPD).⁴² Opron et al. proposed that the enrichment of *Streptococcus*, *Actinobacillus*, and *Actinomyces* in patients with COPD was associated with decreased lung function, greater symptoms, and more severe radiographic manifestations.⁴³ Moreover, *Streptococcus*, *Prevotella*, *Rothia*, *Veillonella*, and *Actinomyces* are the core microbiota in the lung of patients with cystic fibrosis.⁴⁴ Although previous studies have focused on different pulmonary diseases, some shared microbial taxa were identified in this study, indicating a correlation between these microbiota and oxidative stress and inflammation in the lung.

We further categorized patients with pneumoconiosis into stage I and stage III groups based on diagnostic staging, and

subsequently conducted species composition analysis with the healthy controls (Figure S2). LefSe analysis in the pulmonary microbiome between stage I and stage III groups indicated that *Stenotrophomonas*, *Delftia*, and *Butyrivibrio* were enriched in the stage III group compared with those in the healthy controls, but they were nearly absent in the stage I group (Figure S2A,B, LDA score >3). Additionally, we recruited an extra cohort comprising healthy controls and asymptomatic PM-exposed miners to compare their lung microbiota, showing no significant differences in α -diversity, β -diversity, or composition between the two groups (Figure S3). These results suggested that the structure of the pulmonary microbiome not only reflected the presence of the disease but might also play a crucial role in the severity of pneumoconiosis.

3.3. Differences in Gut Microbiome Profile between Healthy Controls and Patients with Pneumoconiosis.

Alterations in respiratory bacteria were evident in pneumoconiosis patients exposed to PMs for long periods; to further investigate whether gut bacterial communities were also altered, fecal specimens were assessed. A total of 1149 and 1453 ASVs were detected in the control and pneumoconiosis groups, respectively, of which 558 were present in both groups and 895 were found only in the pneumoconiosis group (Figure 3A). While α -diversity was not significantly different between the two groups, the divergent β -diversity emphasized an altered composition of gut microbiota in patients with pneumoconiosis (Figure 3B,C).

Different from the pulmonary microbiota, the most predominant bacterial phyla in the gut microbiota were Firmicutes, followed by Bacteroidota, Proteobacteria, Actino-

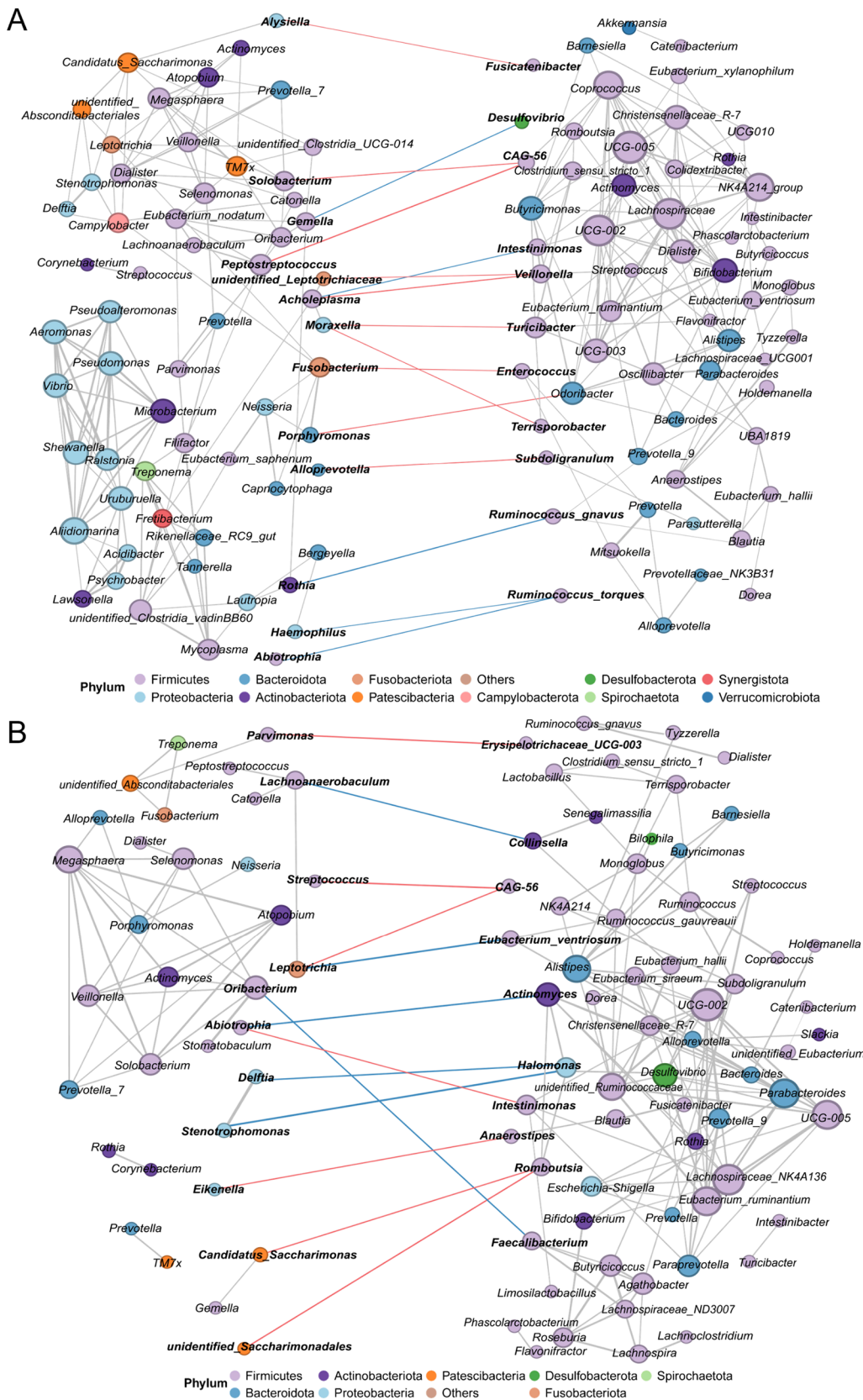


Figure 4. Lung–gut bacterial community interactome in pneumoconiosis. (A, B) The lung–gut interactome networks in (A) control individuals and (B) patients with pneumoconiosis. The left is the network diagram of the lung microbiota, and the right is the network diagram of the gut microbiota. The connecting lines represent the bacterial genera that interact with each other in two ecological niches. Red lines represent positive correlation, while blue lines represent negative correlation. The line width corresponds to the absolute value of the correlation coefficient. Results were filtered according to the threshold criteria of Spearman’s correlation coefficient absolute value $|r| \geq 0.6$ and $P < 0.05$.

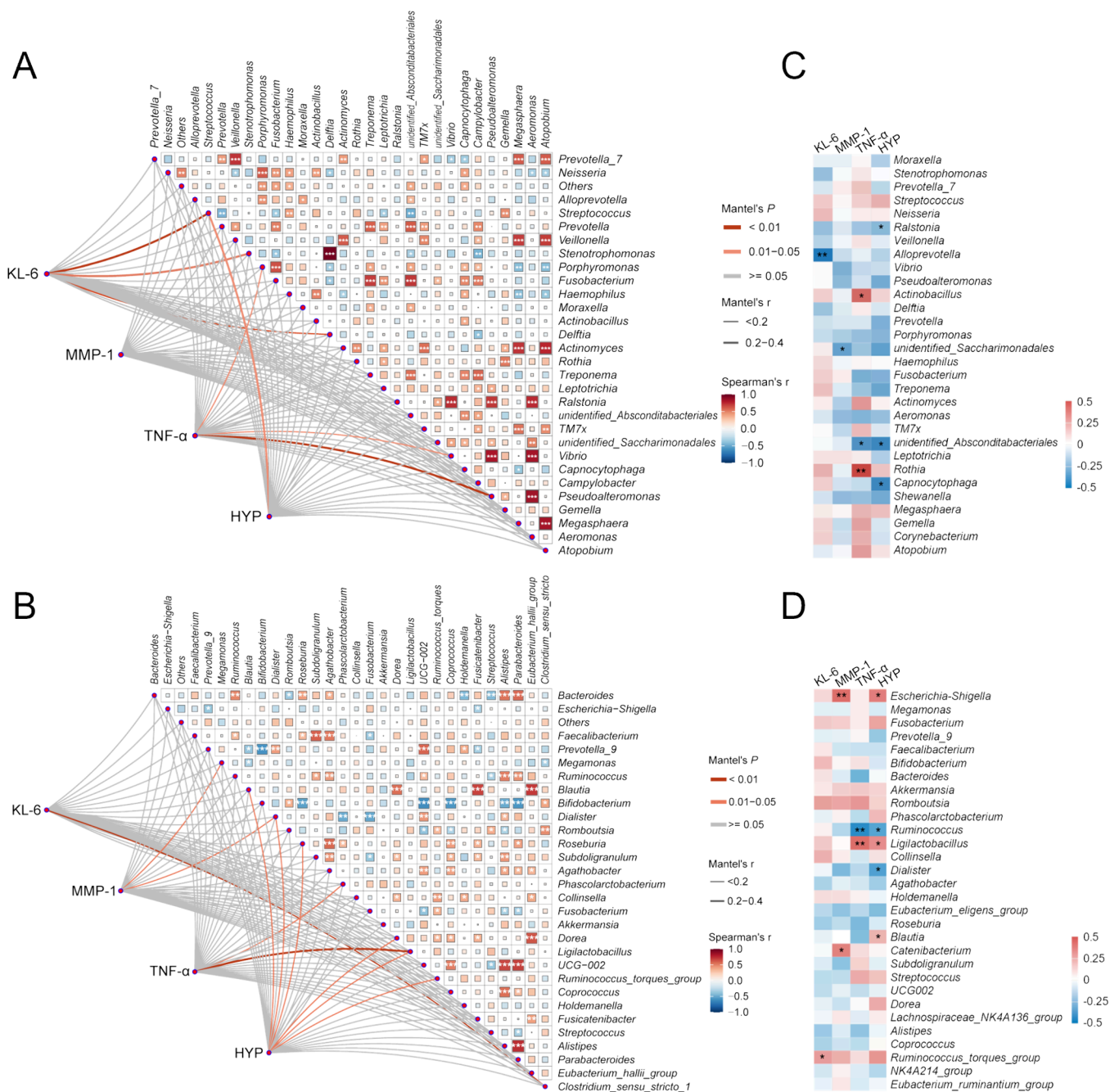


Figure 5. Association between microbial taxa and pneumoconiosis indicators. (A, B) The Mantel test of pneumoconiosis indicators with (A) lung and (B) gut microbiota. (C, D) Heatmaps of the Spearman's correlation between pneumoconiosis indicators and (C) lung and (D) gut microbiota. The color gradient of the heatmap in the triangular part of the figure indicates the change in Spearman's correlation coefficient. The shade of the color represents the value of the correlation coefficients. The edge connections represent the graphical visualization of the Mantel test results. Edge width corresponds to Mantel's r statistic for the corresponding distance correlations, and edge color denotes the statistical significance (Mantel's P). (*) indicates $P < 0.05$, (**) indicates $P < 0.01$.

bacteriota, and Fusobacteriota (Figure 3D). At the genus level, pneumoconiosis patients had enrichment of 9 differential taxa in the gut, whereas only 5 taxa were enriched in the lung. *Escherichia–Shigella*, *Romboutsia*, *Ligilactobacillus*, *Collinsella*, *Phascolarctobacterium*, *Ruminococcus_torques_group*, *Dorea*, *Streptococcus*, and *Ruminococcus_gnavus_group* were more enriched in the gut microbiota of the pneumoconiosis group with significant differences (Figure 3E, LDA score >3). Among the representative taxa in the pneumoconiosis group, *Escherichia–Shigella*, *Ligilactobacillus*, *Phascolarctobacterium*,

and *Streptococcus* were significantly enriched in patients at the stage III (Figure S2C,D, LDA score >3). We also observed an overall similarity and connectivity of the gut microbiota between healthy individuals and asymptomatic PM-exposed miners (Figure S4).

Growing research has demonstrated that the gut microbiome and its metabolic byproducts are involved in modulating systemic inflammation and immune responses, including those that dictate pulmonary health.^{45–48} *Escherichia–Shigella* can release toxins through outer membrane vesicles, which are

associated with mitochondrial apoptosis and NOD-like receptor family and pyrin domain-containing protein 3 (NLRP3) inflammasome activation.⁴⁹ Intestinal *Collinsella* and *Ruminococcus* increase the risk of asthma, possibly because of the involvement of their metabolites in regulating metabolism and immune responses.⁴⁶ Among these genera, *Escherichia–Shigella* belonged to Proteobacteria, *Collinsella* belonged to Actinobacteriota, and all others belonged to Firmicutes. Most genera in Firmicutes are great producers of short-chain fatty acids (SCFAs) and have important effects on intestinal metabolism, host immune signaling, and susceptibility to many lung diseases.⁴⁵ In addition, compared with other phyla, Firmicutes is most closely related to host cytokines and chemokines, including inflammation-related epidermal growth factor and interleukin.⁵⁰

3.4. Microbial Dysbiosis of the Lung–Gut Axis in Pneumoconiosis. After clarifying the composition and taxonomy differences of the lung and gut microbiota, we explored the lung–gut interactions in healthy controls and their alterations in pneumoconiosis individuals through interaction network diagrams (Figure 4). For the healthy controls, there was an outstanding crosstalk between the pulmonary and intestinal microbiota, rather than just an overlap (Figure 4A). Thirteen lung bacteria were involved in the lung–gut interaction, including *Alloprevotella*, *Porphyromonas*, *Fusobacterium*, *Haemophilus*, and other genera. Twelve gut taxa were associated with the lung microbiota, including *Subdoligranulum*, *Fusicatenibacter*, *Lachnospiraceae_CAG_56*, *Lachnospira*, *Ruminococcus*, *Veillonella*, and other genera. These results filled in the knowledge gap regarding the specific microbial taxa responsible for the lung–gut axis interactions in healthy individuals.

In the patients with pneumoconiosis, almost complete alterations were observed in the critical nodes of the lung–gut interaction network diagram, accompanied by an increase in interaction intensity (Figure 4B). There were 11 nodes in the lung: 6 from Firmicutes (such as *Streptococcus*), 2 from Proteobacteria (*Stenotrophomonas* and *Delftia*), 2 from Patescibacteria, and 1 from Fusobacteriota (*Leptotrichia*). There were 10 nodes in the gut microbiota, mainly from Firmicutes, except for 2 from Actinobacteriota (*Collinsella* and *Actinomyces*) and 1 from Proteobacteria (*Halomonas*). The interaction between the pulmonary and intestinal microbiomes was not characterized by the presence of the same bacteria in both sites, but rather by the connections among different taxa. Additionally, Firmicutes played a significant role in the lung–gut interaction; however, the specific mechanisms require further investigation.

There were 4 groups of bacteria with strong correlations (correlation coefficient >0.7), including *Leptotrichia* (lung) and *Eubacterium ventriosum_group* (gut), *Abiotrophia* (lung) and *Actinomyces* (gut), *Delftia* (lung) and *Halomonas* (gut), and *Stenotrophomonas* (lung) and *Halomonas* (gut); all 4 lung taxa were enriched in patients with stage III pneumoconiosis (Figure S2). The enriched pulmonary and intestinal taxa in pneumoconiosis patients became key nodes underlying the lung–gut interaction.

Interaction analyses of lung and gut bacteria were performed within subgroups of stage I and stage III pneumoconiosis patients (Figure S5, Spearman's correlation coefficient absolute value ≥ 0.7 , $P < 0.05$). Compared to the findings in the stage I group (32 positively correlated nodes and 60 negatively correlated nodes), more intersections were observed in the

stage III group (65 positively correlated nodes and 37 negatively correlated nodes), suggesting a stronger lung–gut axis interaction along with disease progression (Figure S5A,B). The theory of “common mucosal immunity” suggests that lymphocytes can migrate between the lung and the gut, leading to a widespread inflammatory response.⁵¹ Studies on animals and humans have indicated that respiratory injuries could affect the dynamics of the gut microbiota, and the microbial ligands and metabolites produced by the intestinal microbiota would shape pulmonary immunity.⁵² This interplay highlights the importance of maintaining a balanced gut microbiome to support respiratory health.

3.5. Lung–Gut Axis Dysbiosis Was Associated with Key Serum Indicators during Pneumoconiosis Progression. We further inspected the relationship between dysbiosis of the pulmonary and intestinal microbiomes with the occurrence and progression of pneumoconiosis. Mantel analysis and Spearman's correlation analysis were combined to identify the critical taxa associated with the inflammatory response and fibrosis during the progression of pneumoconiosis (Figure 5). The changes in KL-6 correlated with *Streptococcus*, *Stenotrophomonas*, *Delftia*, and *Alloprevotella* in the lung, and *Clostridium_sensu_stricto_1* and *Ruminococcus_torques_group* in the gut (Figure 5A,C, $P < 0.05$). Association of MMP-1 in the serum with pulmonary bacteria was not detected, whereas it was strongly associated with *Megamonas*, *Dialister*, *Escherichia–Shigella*, and *Catenibacterium* in the gut (Figure 5B,D, $P < 0.05$).

From the results of the Mantel analysis, there was a correlation between the inflammatory factor TNF- α values and changes in *Porphyromonas*, *Vibrio*, and *Pseudoalteromonas* in the lung ($P < 0.05$). From Spearman's correlation results, TNF- α was positively correlated with *Actinobacillus* and *Rothia* in the lung ($P < 0.05$). For the gut microbiota, *Ligilactobacillus* and *Phascolarctobacterium* were associated with TNF- α , with *Ligilactobacillus* being significantly positively correlated ($P < 0.01$).

The level of HYP, which reflects pulmonary fibrosis, affected the prevalence of 4 taxa in the lung, especially *Streptococcus*; moreover, it correlated with 8 taxa in the intestinal microbiome, including *Blautia*, *Dialister*, *Roseburia*, *Dorea*, *Ligilactobacillus*, *Ruminococcus_torques_group*, *Escherichia–Shigella*, and *Ruminococcus*. Both Mantel and Spearman's analyses suggested the importance of *Ligilactobacillus*, *Blautia*, and *Dialister*. When examining patients in stages I and III, *Stenotrophomonas* and *Delftia* in the lung were associated with HYP, and *Prevotella_7* exhibited a significant correlation with TNF- α (Figure S6, $P < 0.01$). This observation implied that the abundance of these 3 specific taxa could serve as a potential biomarker for the advancement of this disease.

Among the cardinal taxa associated with disease indicators, many of them were involved in lung–gut crosstalk, including *Streptococcus*, *Stenotrophomonas*, *Delftia*, *Alloprevotella*, *Actinobacillus*, and *Rothia* in the lung, as well as *Blautia*, *Ligilactobacillus*, *Dialister*, *Ruminococcus_torques_group*, and *Escherichia–Shigella* in the gut. This observation revealed a correlation between dysregulation of the lung–gut axis and the presence of inflammation and fibrosis. Additionally, we conducted an analysis of the functional changes in the microbiota based on the KEGG (Kyoto Encyclopedia of Genes and Genomes) database (Figure S7). The alterations in lung microbiota functionality resided primarily in metabolic processes, including glycan metabolism, lipid metabolism, and

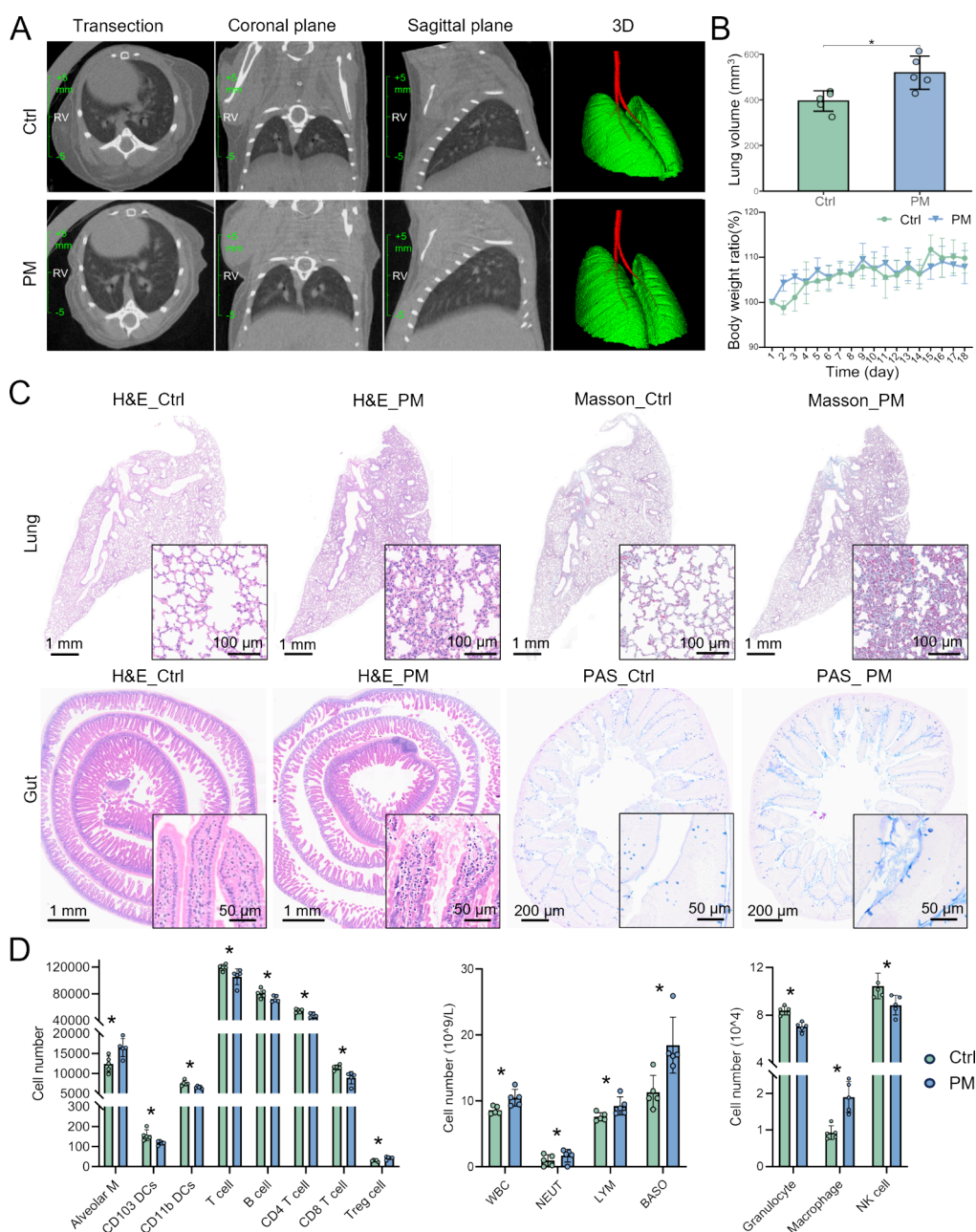


Figure 6. Exposure to inhalable PMs induced systemic inflammatory responses and local tissue damages. (A) Transaction, coronal, sagittal, and 3D CT images of mouse lungs. (B) The change of lung volume and body weight ratio between the control and PM groups. (C) H&E and Masson staining were performed on lung sections from mice; H&E and PAS staining were performed on intestine sections from two groups of mice. (D) The changes in immune cells from the lungs, peripheral blood, and intestines of mice. Ctrl, untreated control mice. PM, PM-exposed mice. (*) indicates $P < 0.05$.

amino acid metabolism. In contrast, the functional changes of gut microbiota were related to metabolism as well as various human diseases, such as small-cell lung cancer and cardiovascular diseases. Our findings together indicated that the changes in the lung–gut microbiota of patients with pneumoconiosis elicited profound implications in overall health.

3.6. Pulmonary and Intestinal Barrier Injury and Systemic Inflammation Occurred in the Animal Model of Pneumoconiosis. Next, we established a mouse model to validate the relationship between the lung–gut axis disruption and systemic inflammation following PM exposure (Figure S8A). The particles predominantly exhibited an irregular block

morphology, with aerodynamic diameters ranging from 0.4 to 4.0 μm that approximated a normal distribution (Figure S8B,C). Elemental analysis revealed that primary constituents of PMs included oxygen (O), Si, carbon (C), Al, and ferrum (Fe), revealing a similar composition to particles in pneumoconiosis patients' BALF (Figure S8D).

The micro-CT results indicated that the lung window of mice in the untreated control group unveiled distinct lung architecture with normal density and distribution (Figure 6A). In contrast, the mice in the PM group appeared hypertrophied lung texture, with multiple ground-glass opacities noted within the lung field, aligning with the pathological characteristics observed in pneumoconiosis patients. Three-dimensional

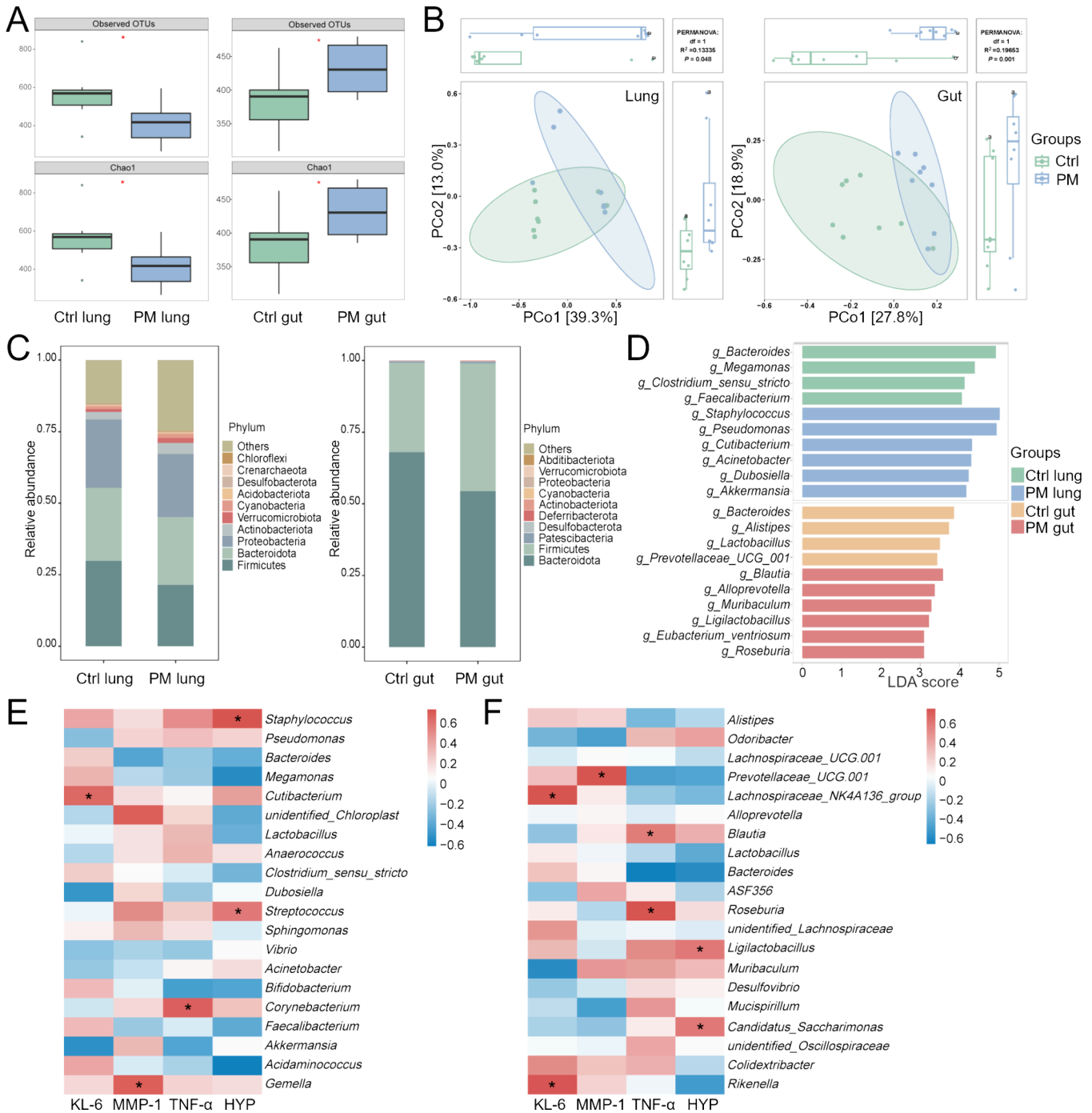


Figure 7. Generalized inflammatory state linked to homeostatic disorders of the lung and gut microbiota. (A) α -Diversity indices (observed OTUs and Chao1) in the lung and gut microbiota. (B) β -Diversity in the lung and gut microbiota. Same superscripts (a and a) indicate no statistical significance, while different superscripts (a and b) indicate statistical significance ($P < 0.05$). (C) Bacterial taxonomic profiles at the phylum level in the lung and gut microbiota. (D) LefSe showing generic taxa that were overrepresented significantly in the lung and gut between control and PM-exposed mice. (E, F) Heatmaps showing Spearman's correlation of pneumoconiosis indicators with (E) lung microbiota and (F) gut microbiota of the two groups of mice. Ctrl, untreated control mice. PM, PM-exposed mice. (*) indicates $P < 0.05$.

images of the lungs were created (Quantum GX2 3D software, PerkinElmer, China), and mice in the PM group exhibited significantly enhanced pulmonary volume (Figure 6B, $P < 0.05$). H&E staining showed that the alveolar structure of mice exposed to inhalable PMs was significantly damaged, with alveolar collapse and inflammatory cell infiltration (Figure 6C). The Masson staining results showed an increase in collagen fibers in the lung tissue of the PM group. The level of HYP in

the serum of mice in the PM group was significantly higher than that in the control group (Figure S9, $P < 0.01$). In addition, the colon of mice exposed to PMs was damaged, as characterized by increased separation of the intestinal villous epithelium from the lamina propria, enlargement of the gap, and detachment of a small number of intestinal villous epithelial cells. The mucus secreted by the goblet cells was

blue in color, and the number of goblet cells was reduced in PM-exposed mice, as evidenced by PAS staining.

We also examined the number of immune cells in the lungs, peripheral blood, and intestines of two groups of mice (Figure 6D). Compared to mice without PM exposure, the lung tissues of PM-exposed mice exhibited increased alveolar macrophages (alveolar M) and regulatory T cells, alongside a reduction in dendritic cells (DCs), B cells, CD4⁺ T cells, and CD8⁺ T cells ($P < 0.05$). Leukocytes (LYM), neutrophils (NEUT), lymphocytes (LYM), and basophils (BASO) were significantly increased in the peripheral blood of the PM group relative to the control group ($P < 0.05$). The number of granulocytes and natural killer (NK) cells in intestinal tissues decreased significantly in the PM group, while the number of macrophages increased significantly ($P < 0.05$). Moreover, changes in peripheral blood immune cells were correlated with the lung and gut microbiota (Figure S10, $P < 0.05$). These results suggested that exposure to PMs triggered pulmonary inflammatory responses and compromised ventilatory function, potentially resulting in systemic and intestinal inflammation that could subsequently give rise to damage to intestinal epithelial structure and intestinal flora.

3.7. Systemic Spillover of Inflammatory Reaction Linked to Alterations in the Lung and Gut Microbiome.

Further, after exposure to inhalable PMs, significant heterogeneity was observed in the microbial profiles of both the lung and gut of mice (Figure 7). The α -diversity of lung microbiota in the PM group decreased, while that of the gut microbiota increased (Figure 7A, $P < 0.05$). PCoA revealed that PMs modulated the β -diversity of the lung and gut microbiota in mice (Figure 7B, $P < 0.05$ and $P < 0.01$, respectively).

The microbial composition of the two groups of mice showed significant differences. At the phylum level, the PM group showed a remarkable decrease in Bacteroidota (gut microbiota) and an increase in Firmicutes (gut microbiota), Actinobacteriota (lung microbiota), and Verrucomicrobiota (lung microbiota), consistent with the results from patients (Figure 7C). At the genus level, 6 genera were increased in the lung of the PM group, including *Staphylococcus*, *Pseudomonas*, *Cutibacterium*, *Acinetobacter*, *Dubosiella*, and *Akkermansia* (Figure 7D). Although these 6 bacteria were not the same as those seen in taxonomic differences in the lung of pneumoconiosis patients, both *Staphylococcus* and *Streptococcus* were in the class Bacilli; *Pseudomonas* and *Acinetobacter*, as well as *Actinobacillus* enriched in pneumoconiosis patients, all belonged to the class Gammaproteobacteria, and both *Cutibacterium* and *Actinomyces* belonged to the class Actinobacteria. In the gut microbiome, *Blautia*, *Alloprevotella*, *Muribaculum*, *Ligilactobacillus*, *Eubacterium ventriosum_group*, and *Roseburia* were significantly enriched in mice of the PM group; the enrichment of *Ligilactobacillus* was consistent with patient data. Our analysis revealed that the representative genera enriched in the gut microbiota after PM exposure predominantly belonged to the Firmicutes phylum. *Blautia*, *Eubacterium ventriosum_group*, and *Roseburia* enriched in the gut of mice in the PM group, in analogy to the serum indicators in patients with pneumoconiosis. When combining the results from humans and mice, Bacteroidota in the gut microbiota decreased after exposure to PMs, while Verrucomicrobiota and Actinobacteriota in the lung microbiota increased. At the genus level, the relative abundance of both *Eubacterium* and *Ligilactobacillus* in the gut microbiota significantly increased. The reduction of Bacteroidota in

pneumoconiosis patients has also been found in previous studies,⁵³ but the combined increase of *Ligilactobacillus* has not yet been reported.

We further explored the interaction between the pulmonary and gut microbiomes of mice and the indicators of pneumoconiosis (Figure 7E,F). The heatmap revealed that *Cutibacterium*, *Gemella*, and *Corynebacterium* in the lung showed positive correlations with KL-6, MMP-1, and TNF- α , respectively ($P < 0.05$). *Staphylococcus* and *Streptococcus* in the pulmonary microbiome were positively correlated with HYP ($P < 0.05$). For the gut microbiota, the relative abundances of *Blautia* and *Roseburia* demonstrated significant positive correlations with TNF- α levels ($P < 0.05$). *Ligilactobacillus* and *Candidatus_Saccharimonas* were significantly positively correlated with HYP ($P < 0.05$). Lung *Streptococcus*, gut *Ligilactobacillus*, gut *Blautia*, and gut *Roseburia* were consistent with results in humans; these taxa were involved in the lung–gut interactions of the pneumoconiosis group and were associated with disease indicators in the serum, indicating their critical role in the progression of pneumoconiosis. Despite the inherent species differences and challenges in directly comparing the results from mice and humans with pneumoconiosis, significant similarities were observed to provide evidence for the linkage of the lung–gut axis disturbed by PM exposure.

4. DISCUSSION

The concept of the lung–gut axis underscores that respiratory tract and digestive tract share a common embryonic origin and exhibit analogous compositions within their mucosal immune systems.^{51,54} These interconnected systems bear bidirectional communication through diverse pathways, encompassing immune regulation, metabolic interactions, and neuroendocrine signaling.⁵⁵ Notably, this cross-site integration forms a sophisticated and interdependent network, wherein their dynamic interplay profoundly influences the maintenance of systemic immune homeostasis and exerts critical regulatory effects on disease pathogenesis and progression.⁵⁶ When we individually analyzed the interaction networks in healthy controls and pneumoconiosis patients, there was an interaction between the pulmonary and gut microbiota, signifying the presence of the lung–gut axis. In the pneumoconiosis group, the key bacteria involved in lung–gut interaction were almost entirely altered from those in healthy controls, manifesting stronger interactions and more involvement of gut bacteria than that of healthy controls, consistent with previous research.²³ Therefore, the lung–gut axis may establish bidirectional cross-organ communication between pulmonary and intestinal systems through mechanisms dictating microbial communities, metabolites, and immune signaling. While its precise mechanisms require further investigation, this axis transcends the traditional single-niche microbial research paradigm, emphasizing the multisystemic health impacts of cross-niche microbial interactions. These findings offer novel perspectives for investigating how microbial networks participate in the pathogenesis of pneumoconiosis, particularly through microbial ectopic colonization, immunotolerance modulation, and metabolite-mediated organ crosstalk.

This study demonstrated that long-term PM exposure induced pulmonary injury and microbial dysbiosis in pneumoconiosis patients and animals, consistent with previous reports.^{18,19,26} O'Dwyer et al.'s experimental data revealed that respiratory dysbiosis preceded and persisted throughout pulmonary fibrotic progression; notably, germ-free mice

exhibited attenuated pulmonary damage compared to conventional mice after bleomycin exposure, providing mechanistic evidence that microbiota necessarily contribute to fibrogenesis.⁵⁷ Inflammation in pneumoconiosis initially occurs in the lung and spreads to the peripheral blood and intestine through a cascade reaction.⁵⁸ Beyond pulmonary toxicities, we have identified particulate-induced intestinal mucosal barrier disruption and gut immune system remodeling. Clinically corroborating these findings, pneumoconiosis patients exhibit altered lung–gut axis microbial crosstalk, with progressively strengthened microbiota correlations between lung and gut during disease progression. Bacteria that played a key role in lung–gut interactions, including *Streptococcus*, *Stenotrophomonas*, and *Delftia* in the lung, as well as *Ligilactobacillus* and *Blautia* in the intestine, correlated with representative pneumoconiosis indicators. According to current understanding, the alteration in microbiota and inflammatory factors is interrelated, involving gut microbiota-derived components and metabolites such as lipopolysaccharides, metabolite trimethylamine N-oxide, and SCFAs, which are the main regulatory factors of the immune and metabolic systems.^{59,60} Preserving the microbial equilibrium in both the lung and gut is therefore essential for combating bacteria, viruses, and environmental pollutants; it also plays a crucial role in alleviating inflammation, preventing excessive mucus production, and ensuring normal physiological function. Collectively, these findings substantiate the pivotal role of the lung–gut axis dysregulation in the pathogenesis of pneumoconiosis. Future investigations will employ longitudinal multiomics profiling to tease out the causal relationships between cross-niche microbial dynamics and disease progression.

Pneumoconiosis exhibits a prolonged latent period and often remains undetected and undiagnosed in its early stage, with some patients progressing to stage III pneumoconiosis at initial diagnosis. Therefore, developing more convenient and sensitive diagnostic methods would facilitate early detection and intervention. Our current study aimed to fill in this significant knowledge gap by recruiting patients with pneumoconiosis through concurrent sampling of the lung and gut. This approach accounted for temporal variability and facilitated a comprehensive analysis across both organ systems. In this study, we demonstrated that long-term exposure to inhalable PMs led to changes in the lung–gut axis microbiota that were associated with pneumoconiosis progression. This study revealed the presence of bacterial genera in both sputum and fecal microbiota that could distinguish pneumoconiosis. Besides, the lung and gut microbial communities of asymptomatic PM-exposed miners were similar to those of the healthy individuals. However, slight changes in the lung and gut microbiota of asymptomatic miners did not necessarily imply the absence of negative impacts on host health. Further analysis identified distinct characteristic genera in patients with stage I and stage III pneumoconiosis. Specifically, *Neisseria* (lung) and *Romboutsia* (gut) were highly enriched in stage I patients, while *Stenotrophomonas* (lung) and *Bacteroides* (gut) were predominantly enriched in stage III patients. Microbiota profiling represents a noninvasive and convenient method, providing novel insights into the development of alternative diagnostic approaches for pneumoconiosis.

In fact, there are certain limitations in this study. First, our sequencing study primarily focused on the bacterial constituents of the lung and gut, while the potential contributions of fungal and viral elements to the overall impact of microbiota

on pulmonary fibrosis cannot be overlooked.⁶¹ In addition, the absence of female pneumoconiosis patients and the relatively small sample size may limit the generalizability of the findings. This study may not have accounted for all confounding factors, such as individual disease heterogeneity, personal psychological state, and dietary preferences, limiting the insights into the underlying variable elements. Furthermore, methodological constraints arise from the observational cross-sectional design. The comparison between the healthy control group and the pneumoconiosis group at a single time point would fail to explain individual heterogeneity and cannot provide strong causal inference. Conducting longitudinal comparisons of the microbiome in the same group of PM-exposed population across different stages from health to pneumoconiosis onset would provide more compelling evidence. Accordingly, changes in the microbiota and related clinical examinations of patients with pneumoconiosis should be tracked in the future, and exploration of the key targets of the lung–gut axis in the progression and treatment of pneumoconiosis is required.

5. CONCLUSIONS

Microbial dysbiosis serves as a crucial mediator for the detrimental effects induced by inhalable PMs. Despite its importance, current understanding of the lung and gut microbiomes in pollution-related diseases remains elusive. This study was committed to shedding light on the crosstalk along the lung–gut axis in pneumoconiosis patients and its relationship with disease onset and progression. Using 16S rRNA sequencing analysis, microbial dysbiosis of the lung and gut niches was observed in pneumoconiosis patients, relative to healthy controls. Besides, Mantel and Spearman's analyses revealed a significant relationship between the dysregulated lung–gut axis and disease indicators (KL-6, MMP-1, TNF- α , and HYP). In the PM-induced systemic inflammatory response, animal studies verified that both the pulmonary and intestinal microbiomes exhibited changes that were further correlated with disease indicators. Through comprehensive analysis of the pneumoconiosis cohort and mouse models, *Streptococcus* and *Stenotrophomonas* in the lung microbiota, along with *Ligilactobacillus* and *Blautia* in the gut microbiota, may represent key microbial communities in deciding disease progression. Overall, this study revealed that inhalable PMs not only induced pulmonary damage but also triggered intestinal inflammation and microbial dysbiosis along the lung–gut axis. Our findings offer new insights into auxiliary diagnosis and pathological mechanisms of pneumoconiosis from a lung–gut axis perspective.

■ ASSOCIATED CONTENT

Supporting Information

The Supporting Information is available free of charge at <https://pubs.acs.org/doi/10.1021/acs.est.5c00798>.

Additional results of characterization of pneumoconiosis indicators and microbiota profiles among stage I and stage III pneumoconiosis patients; the correlation of microbiota with pneumoconiosis indicators in the serum of stage I and stage III pneumoconiosis patients; the lung and gut microbiota diversity and composition of nonexposed healthy controls and asymptomatic PM-exposed miners; functional analysis in lung and gut microbiota of healthy controls and pneumoconiosis

patients; physicochemical characterization of PMs for intranasal exposure in mice; Spearman's correlation of peripheral blood immune cells with the lung and gut microbiota of mice; and the fluorescent dye-conjugated antibodies used in flow cytometry (PDF)

AUTHOR INFORMATION

Corresponding Author

Zheng Dong – Medical Science and Technology Innovation Center and School of Public Health, Shandong First Medical University and Shandong Academy of Medical Sciences, Jinan, Shandong 250117, P. R. China; orcid.org/0009-0008-5210-7455; Email: zdong@sdfmu.edu.cn

Authors

Huimin Ma – Medical Science and Technology Innovation Center and School of Stomatology, Shandong First Medical University and Shandong Academy of Medical Sciences, Jinan, Shandong 250117, P. R. China; Department of Stomatology, Shandong Provincial Hospital affiliated to Shandong First Medical University, Jinan, Shandong 250021, P. R. China; orcid.org/0000-0003-1817-0625

Xu Zhang – Medical Science and Technology Innovation Center and School of Public Health, Shandong First Medical University and Shandong Academy of Medical Sciences, Jinan, Shandong 250117, P. R. China

Ning Li – Medical Science and Technology Innovation Center, Shandong First Medical University and Shandong Academy of Medical Sciences, Jinan, Shandong 250117, P. R. China

Conghe Liu – Medical Science and Technology Innovation Center, Shandong First Medical University and Shandong Academy of Medical Sciences, Jinan, Shandong 250117, P. R. China

Xi Zhou – Shandong Academy of Occupational Health and Occupational Medicine, Occupational Diseases Hospital of Shandong First Medical University, Jinan, Shandong 250062, P. R. China

Jin He – Shandong Academy of Occupational Health and Occupational Medicine, Occupational Diseases Hospital of Shandong First Medical University, Jinan, Shandong 250062, P. R. China

Juan Ma – State Key Laboratory of Environmental Chemistry and Ecotoxicology, Research Center for Eco-Environmental Sciences, Chinese Academy of Sciences, Beijing 100085, P. R. China; University of Chinese Academy of Sciences, Beijing 100049, P. R. China

Shuping Zhang – Medical Science and Technology Innovation Center, Shandong First Medical University and Shandong Academy of Medical Sciences, Jinan, Shandong 250117, P. R. China; orcid.org/0000-0003-1586-0559

Haidong Kan – School of Public Health, Key Lab of Public Health Safety of the Ministry of Education, and NHC Key Lab of Health Technology Assessment, Fudan University, Shanghai 200032, P. R. China; orcid.org/0000-0002-1871-8999

Sijin Liu – Medical Science and Technology Innovation Center, Shandong First Medical University and Shandong Academy of Medical Sciences, Jinan, Shandong 250117, P. R. China; State Key Laboratory of Environmental Chemistry and Ecotoxicology, Research Center for Eco-Environmental Sciences, Chinese Academy of Sciences, Beijing 100085, P. R. China; University of Chinese Academy of Sciences, Beijing 100049, P. R. China; orcid.org/0000-0002-5643-0734

Complete contact information is available at:

<https://pubs.acs.org/10.1021/acs.est.5c00798>

Author Contributions

Z.D., S.L., and H.K. conceived and designed the project; H.M., N.L., and C.L. performed the laboratory experiments; H.M. and X. Zhang performed the analysis of 16S rRNA gene sequencing data; H.M. and N.L. created the abstract graphic; J.H. and X. Zhou were responsible for the patient recruitment and sample collection; Z.D., S.Z., and J.M. viewed and edited the manuscript; H.M. wrote the manuscript with comments from the coauthors.

Notes

The authors declare no competing financial interest.

ACKNOWLEDGMENTS

This work was supported by the National Natural Science Foundation of China (Grants 22406113 and 22422610), the Natural Science Foundation of Shandong Province (Grants ZR2024QB344 and ZR2023QH467), the Joint Innovation Team for Clinical & Basic Research (Grant 202407), the Youth Innovation Promotion Association of Chinese Academy of Sciences (Grant 2022042), and the Major Project of Guangzhou National Laboratory (Grant GZNL2024A01028). We thank all of the pneumoconiosis patients and healthy volunteers for participating in this study.

REFERENCES

- (1) Wang, Z.; Yan, J.; Zhang, P.; Li, Z.; Guo, C.; Wu, K.; Li, X.; Zhu, X.; Sun, Z.; Wei, Y. Chemical characterization, source apportionment, and health risk assessment of PM_{2.5} in a typical industrial region in North China. *Environ. Sci. Pollut. Res. Int.* **2022**, *29* (47), 71696–71708.
- (2) Sharma, S. K.; Mukherjee, S.; Choudhary, N.; Rai, A.; Ghosh, A.; Chatterjee, A.; Vijayan, N.; Mandal, T. K. Seasonal variation and sources of carbonaceous species and elements in PM_{2.5} and PM₁₀ over the eastern Himalaya. *Environ. Sci. Pollut. Res. Int.* **2021**, *28* (37), 51642–51656.
- (3) Xia, T.; Zhu, Y.; Mu, L.; Zhang, Z. F.; Liu, S. Pulmonary diseases induced by ambient ultrafine and engineered nanoparticles in twenty-first century. *Natl. Sci. Rev.* **2016**, *3* (4), 416–429.
- (4) Zaręba, Ł.; Piszczatowska, K.; Dżaman, K.; Soroczynska, K.; Motamedi, P.; Szczepański, M. J.; Ludwig, N. The Relationship between Fine Particle Matter (PM_{2.5}) Exposure and Upper Respiratory Tract Diseases. *J. Pers. Med.* **2024**, *14* (1), No. 98.
- (5) Qiu, J.; Ma, J.; Dong, Z.; Ren, Q.; Shan, Q.; Liu, J.; Gao, M.; Liu, G.; Zhang, S.; Qu, G.; Jiang, G.; Liu, S. Lung megakaryocytes engulf inhaled airborne particles to promote intrapulmonary inflammation and extrapulmonary distribution. *Nat. Commun.* **2024**, *15* (1), 7396.
- (6) Cohen, R. A.; Petsonk, E. L.; Rose, C.; Young, B.; Regier, M.; Najmuddin, A.; Abraham, J. L.; Churg, A.; Green, F. H. Lung Pathology in U.S. Coal Workers with Rapidly Progressive Pneumoconiosis Implicates Silica and Silicates. *Am. J. Respir. Crit. Care Med.* **2016**, *193* (6), 673–680.
- (7) Hua, J. T.; Cool, C. D.; Green, F. H. Y. Pathology and Mineralogy of the Pneumoconioses. *Semin. Respir. Crit. Care Med.* **2023**, *44* (3), 327–339.
- (8) Ma, H.; Dong, Z.; Zhang, X.; Liu, C.; Liu, Z.; Zhou, X.; He, J.; Zhang, S. Airway bacterial microbiome signatures correlate with occupational pneumoconiosis progression. *Ecotoxicol. Environ. Saf.* **2024**, *284*, 116875.
- (9) The Human Microbiome Project Consortium. Structure, function and diversity of the healthy human microbiome. *Nature* **2012**, *486* (7402), 207–214.

- (10) Ahrobia, T.; Das, S.; Bakshi, S.; Das, B. Structure, functions, and diversity of the healthy human microbiome. *Prog. Mol. Biol. Transl. Sci.* **2022**, *191* (1), 53–82.
- (11) Jia, D.; Wang, Q.; Qi, Y.; Jiang, Y.; He, J.; Lin, Y.; Sun, Y.; Xu, J.; Chen, W.; Fan, L.; Yan, R.; Zhang, W.; Ren, G.; Xu, C.; Ge, Q.; Wang, L.; Liu, W.; Xu, F.; Wu, P.; Wang, Y.; Chen, S.; Wang, L. Microbial metabolite enhances immunotherapy efficacy by modulating T cell stemness in pan-cancer. *Cell* **2024**, *187* (7), 1651–1665.
- (12) Arifuzzaman, M.; Collins, N.; Guo, C. J.; Artis, D. Nutritional regulation of microbiota-derived metabolites: Implications for immunity and inflammation. *Immunity* **2024**, *57* (1), 14–27.
- (13) Lynch, S. V.; Pedersen, O. The Human Intestinal Microbiome in Health and Disease. *N. Engl. J. Med.* **2016**, *375* (24), 2369–2379.
- (14) Hegelmaier, T.; Lebbing, M.; Duscha, A.; Tomaske, L.; Tönges, L.; Holm, J. B.; Björn Nielsen, H.; Gatermann, S. G.; Przuntek, H.; Haghikia, A. Interventional Influence of the Intestinal Microbiome Through Dietary Intervention and Bowel Cleansing Might Improve Motor Symptoms in Parkinson's Disease. *Cells* **2020**, *9* (2), No. 376.
- (15) Pragman, A. A.; Lyu, T.; Baller, J. A.; Gould, T. J.; Kelly, R. F.; Reilly, C. S.; Isaacson, R. E.; Wendt, C. H. The lung tissue microbiota of mild and moderate chronic obstructive pulmonary disease. *Microbiome* **2018**, *6* (1), No. 7.
- (16) Enamorado, M.; Kulalert, W.; Han, S. J.; Rao, I.; Delaleu, J.; Link, V. M.; Yong, D.; Smelkinson, M.; Gil, L.; Nakajima, S.; Linehan, J. L.; Bouladoux, N.; Wlaschin, J.; Kabat, J.; Kamenyeva, O.; Deng, L.; Gribovnik, I.; Chesler, A. T.; Chiu, I. M.; Le Pichon, C. E.; Belkaid, Y. Immunity to the microbiota promotes sensory neuron regeneration. *Cell* **2023**, *186* (3), 607–620.
- (17) Wu, Y.; Li, H.; Xu, D.; Li, H.; Chen, Z.; Cheng, Y.; Yin, G.; Niu, Y.; Liu, C.; Kan, H.; Yu, D.; Chen, R. Associations of fine particulate matter and its constituents with airway inflammation, lung function, and buccal mucosa microbiota in children. *Sci. Total Environ.* **2021**, *773*, 145619.
- (18) Zhang, J.; Cheng, H.; Di Narzo, A.; Zhu, Y.; Xie, S.; Shao, X.; Zhang, Z.; Chung, S. K.; Hao, K. Profiling Microbiota from Multiple Sites in the Respiratory Tract to Identify a Biomarker for PM(2.5) Nitrate Exposure-Induced Pulmonary Damages. *Environ. Sci. Technol.* **2023**, *57* (19), 7346–7357.
- (19) Wang, S.; Zhou, Q.; Tian, Y.; Hu, X. The Lung Microbiota Affects Pulmonary Inflammation and Oxidative Stress Induced by PM(2.5) Exposure. *Environ. Sci. Technol.* **2022**, *56* (17), 12368–12379.
- (20) Ran, Z.; Yang, J.; Liu, L.; Wu, S.; An, Y.; Hou, W.; Cheng, T.; Zhang, Y.; Zhang, Y.; Huang, Y.; Zhang, Q.; Wan, J.; Li, X.; Xing, B.; Ye, Y.; Xu, P.; Chen, Z.; Zhao, J.; Li, R. Chronic PM(2.5) exposure disrupts intestinal barrier integrity via microbial dysbiosis-triggered TLR2/5-MyD88-NLRP3 inflammasome activation. *Environ. Res.* **2024**, *258*, 119415.
- (21) Qiu, T.; Fang, Q.; Zeng, X.; Zhang, X.; Fan, X.; Zang, T.; Cao, Y.; Tu, Y.; Li, Y.; Bai, J.; Huang, J.; Liu, Y. Short-term exposures to PM(2.5), PM(2.5) chemical components, and antenatal depression: Exploring the mediating roles of gut microbiota and fecal short-chain fatty acids. *Ecotoxicol. Environ. Saf.* **2024**, *277*, 116398.
- (22) Campolim, C. M.; Weissmann, L.; Ferreira, C. K. O.; Zordão, O. P.; Dornellas, A. P. S.; de Castro, G.; Zanotto, T. M.; Boico, V. F.; Quaresma, P. G. F.; Lima, R. P. A.; Donato, J., Jr.; Veras, M. M.; Saldiva, P. H. N.; Kim, Y. B.; Prada, P. O. Short-term exposure to air pollution (PM(2.5)) induces hypothalamic inflammation, and long-term leads to leptin resistance and obesity via Tlr4/Ikbke in mice. *Sci. Rep.* **2020**, *10* (1), 10160.
- (23) Narayana, J. K.; Aliberti, S.; Mac Aogáin, M.; Jaggi, T. K.; Ali, N.; Ivan, F. X.; Cheng, H. S.; Yip, Y. S.; Vos, M. I. G.; Low, Z. S.; Lee, J. X. T.; Amati, F.; Gramegna, A.; Wong, S. H.; Sung, J. J. Y.; Tan, N. S.; Tsaneva-Atanasova, K.; Blasi, F.; Chotirmall, S. H. Microbial Dysregulation of the Gut-Lung Axis in Bronchiectasis. *Am. J. Respir. Crit. Care Med.* **2023**, *207* (7), 908–920.
- (24) Chioma, O. S.; Mallott, E. K.; Chapman, A.; Van Amburg, J. C.; Wu, H.; Shah-Gandhi, B.; Dey, N.; Kirkland, M. E.; Blanca Piazuelo, M.; Johnson, J.; Bernard, G. R.; Bodduluri, S. R.; Davison, S.; Haribabu, B.; Bordenstein, S. R.; Drake, W. P. Gut microbiota modulates lung fibrosis severity following acute lung injury in mice. *Commun. Biol.* **2022**, *5* (1), 1401.
- (25) Liang, W.; Yang, Y.; Gong, S.; Wei, M.; Ma, Y.; Feng, R.; Gao, J.; Liu, X.; Tu, F.; Ma, W.; Yi, X.; Liang, Z.; Wang, F.; Wang, L.; Chen, D.; Shu, W.; Miller, B. E.; Tal-Singer, R.; Donaldson, G. C.; Wedzicha, J. A.; Singh, D.; Wilkinson, T. M. A.; Brightling, C. E.; Chen, R.; Zhong, N.; Wang, Z. Airway dysbiosis accelerates lung function decline in chronic obstructive pulmonary disease. *Cell Host Microbe* **2023**, *31* (6), 1054–1070.
- (26) Huo, C.; Jiao, X.; Wang, Y.; Jiang, Q.; Ning, F.; Wang, J.; Jia, Q.; Zhu, Z.; Tian, L. Silica aggravates pulmonary fibrosis through disrupting lung microbiota and amino acid metabolites. *Sci. Total Environ.* **2024**, *945*, 174028.
- (27) Ren, Q.; Ma, J.; Li, X.; Meng, Q.; Wu, S.; Xie, Y.; Qi, Y.; Liu, S.; Chen, R. Intestinal Toxicity of Metal Nanoparticles: Silver Nanoparticles Disorder the Intestinal Immune Microenvironment. *ACS Appl. Mater. Interfaces* **2023**, *15* (23), 27774–27788.
- (28) Dong, Z.; Ma, J.; Qiu, J.; Ren, Q.; Shan, Q.; Duan, X.; Li, G.; Zuo, Y. Y.; Qi, Y.; Liu, Y.; Liu, G.; Lynch, L.; Fang, M.; Liu, S. Airborne fine particles drive H1N1 viruses deep into the lower respiratory tract and distant organs. *Sci. Adv.* **2023**, *9* (23), eadf2165.
- (29) Ma, J.; Liu, X.; Yang, Y.; Qiu, J.; Dong, Z.; Ren, Q.; Zuo, Y. Y.; Xia, T.; Chen, W.; Liu, S. Binding of Benzo[a]pyrene Alters the Bioreactivity of Fine Biochar Particles toward Macrophages Leading to Deregulated Macrophagic Defense and Autophagy. *ACS Nano* **2021**, *15* (6), 9717–9731.
- (30) Deissová, T.; Zapletalová, M.; Kunovský, L.; Kroupa, R.; Grolich, T.; Kala, Z.; Bořilová Linhartová, P.; Lochman, J. 16S rRNA gene primer choice impacts off-target amplification in human gastrointestinal tract biopsies and microbiome profiling. *Sci. Rep.* **2023**, *13* (1), 12577.
- (31) Hall, M.; Beiko, R. G. 16S rRNA Gene Analysis with QIIME2. *Methods Mol. Biol.* **2018**, *1849*, 113–129.
- (32) Lima, J.; Manning, T.; Rutherford, K. M.; Baima, E. T.; Dewhurst, R. J.; Walsh, P.; Roehe, R. Taxonomic annotation of 16S rRNA sequences of pig intestinal samples using MG-RAST and QIIME2 generated different microbiota compositions. *J. Microbiol. Methods* **2021**, *186*, 106235.
- (33) Segata, N.; Izard, J.; Waldron, L.; Gevers, D.; Miropolsky, L.; Garrett, W. S.; Huttenhower, C. Metagenomic biomarker discovery and explanation. *Genome Biol.* **2011**, *12* (6), R60.
- (34) Hou, Z.; Zhang, X.; Gao, Y.; Geng, J.; Jiang, Y.; Dai, H.; Wang, C. Serum Osteopontin, KL-6, and Syndecan-4 as Potential Biomarkers in the Diagnosis of Coal Workers' Pneumoconiosis: A Case-Control Study. *Pharmgenomics Pers. Med.* **2023**, *16*, 537–549.
- (35) Kumari, S.; Singh, R. Protective effects of intranasal curcumin on silica-induced lung damage. *Cytokine* **2022**, *157*, 155949.
- (36) Vanka, K. S.; Shukla, S.; Gomez, H. M.; James, C.; Palanisami, T.; Williams, K.; Chambers, D. C.; Britton, W. J.; Ilic, D.; Hansbro, P. M.; Horvat, J. C. Understanding the pathogenesis of occupational coal and silica dust-associated lung disease. *Eur. Respir. Rev.* **2022**, *31* (165), No. 210250.
- (37) Hu, Y.; Wang, L. S.; Jin, Y. P.; Du, S. S.; Du, Y. K.; He, X.; Weng, D.; Zhou, Y.; Li, Q. H.; Shen, L.; Zhang, F.; Su, Y. L.; Sun, X. L.; Ding, J. J.; Zhang, W. H.; Cai, H. R.; Dai, H. P.; Dai, J. H.; Li, H. P. Serum Krebs von den Lungen-6 level as a diagnostic biomarker for interstitial lung disease in Chinese patients. *Clin. Respir. J.* **2017**, *11* (3), 337–345.
- (38) Helal, M. G.; Said, E. Carvedilol attenuates experimentally induced silicosis in rats via modulation of P-AKT/mTOR/TGFβ1 signaling. *Int. Immunopharmacol.* **2019**, *70*, 47–55.
- (39) Sullivan, D. E.; Ferris, M.; Pociask, D.; Brody, A. R. The latent form of TGFβ(1) is induced by TNFα through an ERK specific pathway and is activated by asbestos-derived reactive oxygen species in vitro and in vivo. *J. Immunotoxicol.* **2008**, *5* (2), 145–149.
- (40) Ma, H.; Dong, Z.; Zhang, X.; Liu, C.; Liu, Z.; Zhou, X.; He, J.; Zhang, S. Airway bacterial microbiome signatures correlate with

occupational pneumoconiosis progression. *Ecotoxicol. Environ. Saf.* **2024**, *284*, 116875.

(41) Callahan, B. J.; McMurdie, P. J.; Rosen, M. J.; Han, A. W.; Johnson, A. J. A.; Holmes, S. P. DADA2: High-resolution sample inference from Illumina amplicon data. *Nat. Methods* **2016**, *13* (7), 581–583.

(42) Lin, L.; Yi, X.; Liu, H.; Meng, R.; Li, S.; Liu, X.; Yang, J.; Xu, Y.; Li, C.; Wang, Y.; Xiao, N.; Li, H.; Liu, Z.; Xiang, Z.; Shu, W.; Guan, W. J.; Zheng, X. Y.; Sun, J.; Wang, Z. The airway microbiome mediates the interaction between environmental exposure and respiratory health in humans. *Nat. Med.* **2023**, *29* (7), 1750–1759.

(43) Opron, K.; Begley, L. A.; Erb-Downward, J. R.; Li, G.; Alexis, N. E.; Barjaktarevic, I.; Barr, R. G.; Bleecker, E. R.; Boucher, R.; Bowler, R. P.; et al. Loss of Airway Phylogenetic Diversity Is Associated with Clinical and Pathobiological Markers of Disease Development in Chronic Obstructive Pulmonary Disease. *Am. J. Respir. Crit. Care Med.* **2024**, *210* (2), 186–200.

(44) Coburn, B.; Wang, P. W.; Diaz Caballero, J.; Clark, S. T.; Brahma, V.; Donaldson, S.; Zhang, Y.; Surendra, A.; Gong, Y.; Elizabeth Tullis, D.; Yau, Y. C.; Waters, V. J.; Hwang, D. M.; Guttman, D. S. Lung microbiota across age and disease stage in cystic fibrosis. *Sci. Rep.* **2015**, *5*, 10241.

(45) Ashique, S.; De Rubis, G.; Sirohi, E.; Mishra, N.; Rihan, M.; Garg, A.; Reyes, R. J.; Manandhar, B.; Bhatt, S.; Jha, N. K.; Singh, T. G.; Gupta, G.; Singh, S. K.; Chellappan, D. K.; Paudel, K. R.; Hansbro, P. M.; Oliver, B. G.; Dua, K. Short Chain Fatty Acids: Fundamental mediators of the gut-lung axis and their involvement in pulmonary diseases. *Chem. Biol. Interact.* **2022**, *368*, 110231.

(46) Li, R.; Guo, Q.; Zhao, J.; Kang, W.; Lu, R.; Long, Z.; Huang, L.; Chen, Y.; Zhao, A.; Wu, J.; Yin, Y.; Li, S. Assessing causal relationships between gut microbiota and asthma: evidence from two sample Mendelian randomization analysis. *Front. Immunol.* **2023**, *14*, No. 1148684.

(47) Dang, A. T.; Marsland, B. J. Microbes, metabolites, and the gut-lung axis. *Mucosal Immunol.* **2019**, *12* (4), 843–850.

(48) Liu, H.; Wang, G.; Zhang, J.; Lu, B.; Li, D.; Chen, J. Inhalation of diesel exhaust particulate matter accelerates weight gain via regulation of hypothalamic appetite-related genes and gut microbiota metabolism. *J. Hazard. Mater.* **2024**, *466*, 133570.

(49) Deo, P.; Chow, S. H.; Han, M. L.; Speir, M.; Huang, C.; Schittenhelm, R. B.; Dhital, S.; Emery, J.; Li, J.; Kile, B. T.; Vince, J. E.; Lawlor, K. E.; Naderer, T. Mitochondrial dysfunction caused by outer membrane vesicles from Gram-negative bacteria activates intrinsic apoptosis and inflammation. *Nat. Microbiol.* **2020**, *5* (11), 1418–1427.

(50) Zhou, X.; Shen, X.; Johnson, J. S.; Spakowicz, D. J.; Agnello, M.; Zhou, W.; Avina, M.; Honkala, A.; Chleilat, F.; Chen, S. J.; Cha, K.; Leopold, S.; Zhu, C.; Chen, L.; Lyu, L.; Hornburg, D.; Wu, S.; Zhang, X.; Jiang, C.; Jiang, L.; Jiang, L.; Jian, R.; Brooks, A. W.; Wang, M.; Contrepolis, K.; Gao, P.; Rose, S. M. S.-F.; Tran, T. D. B.; Nguyen, H.; Celli, A.; Hong, B.-Y.; Bautista, E. J.; Dorsett, Y.; Kavathas, P. B.; Zhou, Y.; Sodergren, E.; Weinstock, G. M.; Snyder, M. P. Longitudinal profiling of the microbiome at four body sites reveals core stability and individualized dynamics during health and disease. *Cell Host Microbe* **2024**, *32* (4), 506–526.

(51) Mestecky, J. The common mucosal immune system and current strategies for induction of immune responses in external secretions. *J. Clin. Immunol.* **1987**, *7* (4), 265–276.

(52) Özçam, M.; Lynch, S. V. The gut-airway microbiome axis in health and respiratory diseases. *Nat. Rev. Microbiol.* **2024**, *22* (8), 492–506.

(53) Zhou, Y.; Chen, L.; Sun, G.; Li, Y.; Huang, R. Alterations in the gut microbiota of patients with silica-induced pulmonary fibrosis. *J. Occup. Med. Toxicol.* **2019**, *14*, No. 5.

(54) Georgiou, K.; Marinov, B.; Farooqi, A. A.; Gazouli, M. Gut Microbiota in Lung Cancer: Where Do We Stand? *Int. J. Mol. Sci.* **2021**, *22* (19), 10429.

(55) Wang, L.; Cai, Y.; Garssen, J.; Henricks, P. A. J.; Folkerts, G.; Braber, S. The Bidirectional Gut-Lung Axis in Chronic Obstructive

Pulmonary Disease. *Am. J. Respir. Crit. Care Med.* **2023**, *207* (9), 1145–1160.

(56) Cheng, T.-Y.; Chang, C.-C.; Luo, C.-S.; Chen, K.-Y.; Yeh, Y.-K.; Zheng, J.-Q.; Wu, S.-M. Targeting Lung-Gut Axis for Regulating Pollution Particle-Mediated Inflammation and Metabolic Disorders. *Cells* **2023**, *12* (6), No. 901.

(57) O'Dwyer, D. N.; Ashley, S. L.; Gurczynski, S. J.; Xia, M.; Wilke, C.; Falkowski, N. R.; Norman, K. C.; Arnold, K. B.; Huffnagle, G. B.; Salisbury, M. L.; Han, M. K.; Flaherty, K. R.; White, E. S.; Martinez, F. J.; Erb-Downward, J. R.; Murray, S.; Moore, B. B.; Dickson, R. P. Lung Microbiota Contribute to Pulmonary Inflammation and Disease Progression in Pulmonary Fibrosis. *Am. J. Respir. Crit. Care Med.* **2019**, *199* (9), 1127–1138.

(58) Tan, S.; Chen, S. The Mechanism and Effect of Autophagy, Apoptosis, and Pyroptosis on the Progression of Silicosis. *Int. J. Mol. Sci.* **2021**, *22* (15), 8110.

(59) Liu, Q.; Tian, X.; Maruyama, D.; Arjomandi, M.; Prakash, A. Lung immune tone via gut-lung axis: gut-derived LPS and short-chain fatty acids' immunometabolic regulation of lung IL-1 β , FFAR2, and FFAR3 expression. *Am. J. Physiol.: Lung Cell. Mol. Physiol.* **2021**, *321* (1), L65–L78.

(60) Yang, Y.; Zeng, Q.; Gao, J.; Yang, B.; Zhou, J.; Li, K.; Li, L.; Wang, A.; Li, X.; Liu, Z.; Luo, Q.; Zhao, Z.; Liu, B.; Xue, J.; Jiang, X.; Konerman, M. C.; Zheng, L.; Xiong, C. High-circulating gut microbiota-dependent metabolite trimethylamine N-oxide is associated with poor prognosis in pulmonary arterial hypertension. *Eur. Heart J. Open* **2022**, *2* (5), No. oeac021.

(61) Spagnolo, P.; Molyneaux, P. L.; Bernardinello, N.; Cocconcelli, E.; Biondini, D.; Fracasso, F.; Tiné, M.; Saetta, M.; Maher, T. M.; Balestro, E. The Role of the Lung's Microbiome in the Pathogenesis and Progression of Idiopathic Pulmonary Fibrosis. *Int. J. Mol. Sci.* **2019**, *20* (22), No. 5618.